Original Article
Improving anti-tumor outcomes for colorectal cancer therapy through *in situ* thermosensitive gel loading harmine

Zhenzhen Li[1,2,4], Liqing Chen[2], Chenghui He[4], Ying Han[2], Mingfeng Han[2], Yingying Zhang[2], Lingling Qi[2], Xuezhong Xing[3], Wei Huang[2], Zhonggao Gao[2], Jianguo Xing[4]

[1]Key Laboratory of Xinjiang Endemic Phytomedicine Resources of Ministry of Education, School of Pharmacy, Shihezi University, Shihezi 832003, China; [2]State Key Laboratory of Bioactive Substance and Function of Natural Medicines, Department of Pharmaceutics, Institute of Materia Medica, Chinese Academy of Medical Sciences and Peking Union Medical College, Beijing 100050, China; [3]National Cancer Center/National Clinical Research Center for Cancer/Cancer Hospital, Chinese Academy of Medical Sciences and Peking Union Medical College, Beijing 100021, China; [4]Xinjiang Key Laboratory of Uighur Medicines, Xinjiang Institute of Materia Medica, Urumqi 830004, China

Abstract: Colorectal cancer is a common malignant tumor that seriously endangers human health. Harmine (HM), a natural product, has been shown to have a significant inhibitory effect on various cancers. However, systemic injection of HM can cause central nervous toxicity, which limits its clinical application. Local administration of HM overcomes this problem to a certain extent. In this study, we prepared an *in situ* thermosensitive HM gel preparation (HM gel), and used it to treat colon cancer with reduced toxic side effects and prolonged residence time of HM at the tumor site. We employed a central composite design and response surface methodology to optimize the formulation, and evaluated the physicochemical properties, rectal retention capacity, and *in vitro* and *in vivo* anti-tumor effects of HM gel on colon 26 tumor cells. The results showed that HM gel had a significant inhibitory effect on the growth of colon 26 cells *in vitro*. In an orthotopic tumor-bearing mouse model, HM gel exhibited an obvious inhibitory effect on tumor growth and metastasis, and significantly prolonged the survival period. In conclusion, HM gel exhibited significant anti-tumor effects on colon cancer, and therefore presents a promising formulation for the treatment of colorectal cancer.

Keywords: Colorectal cancer, harmine, *in situ* gel, cancer therapy

Introduction

Colorectal cancer is one of the most common malignant tumors worldwide [1], with some of the highest morbidity and mortality rates of all malignant tumors. Moreover, most patients with colorectal cancer are diagnosed in the middle or late stages, and so patient survival is reduced due to metastasis and drug resistance. Recently, with development of early diagnosis technology, new adjuvant therapy concepts, and the application of local drug administration, colorectal cancer treatment has become more standardized, more individualized, and more accurate [2]. With good tolerance and fewer side effects, *in situ* drug therapy could greatly improve the therapeutic effect on colorectal cancer and therefore is an important developmental area for colorectal cancer drug therapy [3].

Peganum harmala L. is a perennial herb of the family Zygophyllaceae, commonly known as 'Harmal', which has a wide range of pharmacological effects on the central nervous system, cardiovascular system, muscle, and ion channels [4]. Harmine (HM) is a β-carboline alkaloid extracted from the seeds of *P. harmala*. HM can inhibit cellular and humoral immunity and monoamine oxidase, and exhibits antitumor, anti-inflammatory, analgesic, antipruritic, and anti-psoriasis effects [5]. The potent an-

titumor effects of HM have been widely studied due to its broad antitumor spectrum. HM has been shown to have an inhibitory effect on cervical cancer, gastric cancer, liver cancer, nasopharyngeal cancer, pancreatic cancer, leukemia, colorectal cancer, and other tumors [6, 7]. However, HM can have serious toxic side effects on the central nervous system, including tremor, convulsion, excitation, and subsequent neural inhibition, which limits the clinical application and development of HM [8]. Development of a local HM administration method could enhance the efficacy on local lesions and simultaneously reduce the central nervous system side effects, and facilitate clinical application of HM tumor therapy.

In situ gel is a local drug delivery system with many useful applications. The formation mechanism of *in situ* gels involves the use of polymer materials that respond to external stimuli (such as temperature, ionic strength, or pH), such that the polymer disperses or conforms under specific physiological conditions. This transformation from solution to semisolid gel state facilitates controlled localized release of drugs contained in the polymer solution [9]. *In situ* gel prepared with water-soluble polymer materials has a highly hydrophilic three-dimensional mesh structure, good histocompatibility and bioadhesion, and unique solution to semisolid gel (sol-gel) transition properties [10]. Additional advantages include the simple preparation process, convenient application, and long retention at application sites, for example injection site, nasal, oral and vaginal mucosa, and mucous membranes including rectal. This confers an advantage over the current *in situ* dosage forms for treatment of colorectal cancer, as enema is not easily retained in the rectum, and suppository form limits the drug distribution area [11]. *In situ* gel can be rapidly gelated in the rectum to adhere to the administration site, preventing drug leakage, and achieving targeted drug delivery. In combination with a long retention time, this significantly improves the convenience of drug administration and exposure.

In order to avoid the side effects associated with systemic HM administration and prolong the retention time of HM in the rectum, we prepared an *in situ* thermosensitive HM gel preparation (HM gel), in which the sol-gel transition occurs immediately at rectal temperature. We then used a central composite design and response surface methodology (CCD-RSM) to optimize the formulation parameters of HM gel, and evaluated its physicochemical properties and *in vivo* rectal retention properties. In addition, we evaluated the *in vitro* and *in vivo* antitumor effects of HM gel using colon 26 tumor cells.

Materials and methods

Materials

Harmine hydrochloride (purity: 98%), 2,2,2-tribromoethanol, and methylene blue trihydrate were purchased from J&K Scientific Ltd. (Beijing, China). P407 and P188 were purchased from BASF SE (Ludwigshafen, Germany). HPMC E5 was purchased from Huzhou Zhanwang Pharmaceutical Co., Ltd. (Zhejiang, China). Benzalkonium bromide was purchased from Nanchang Baiyun Pharmaceutical Co., Ltd (Nanchang, China). Tert-Amyl alcohol was purchased from TCI (Shanghai, China) Development Co., Ltd. (Shanghai, China). Formaldehyde (40%) was purchased from Tianjin Damao Chemical Reagent Factory (Tianjin, China). Methanol was purchased from Thermo Fisher Scientific (Waltham, MA, USA). The TUNEL-POD kit was purchased from Hoffman-La Roche Ltd. (Basel, Switzerland). Annexin V-FITC/PI apoptosis detection kit was purchased from KeyGEN BioTech (Nanjing, China). Cell Counting Kit-8 (CCK-8) was purchased from Dojindo Molecular Technologies (Kumamoto, Japan).

Cell culture

The mouse colon 26 cell line was supplied by the Cell Culture Center of the Institute of Basic Medical Sciences at the Chinese Academy of Medical Sciences. Colon 26 cells were cultured in RPMI 1640 containing 10% FBS in a 5% CO_2 humidified incubator at 37°C. The medium was supplemented with 100 units/mL penicillin and 100 μg/mL streptomycin.

Preparation of HM in situ gels

The HM gel was prepared using a cold method [12]. 1.2% (w/v) HM and right amount of hydroxypropyl methylcellulose (HPMC), Poloxa-

mer 188 (P188), and Poloxamer 407 (P407) were sequentially mixed with 0.02% (w/v) benzalkonium bromide (a preservative agent) with continuous agitation until completely dissolved. Water was added to the full amount and the gel stored at 4°C for 24 h until clarified.

Measurement of the gelation temperature

Gelation temperature was measured using the reverse tube method [13]. A thermometer was placed in a test tube containing 4 mL gel solution in a constant temperature water bath at (37 ± 0.5°C). The test tube was reversed every 30 s to observe gelation. The gelation temperature was recorded when the gel in the reverse tube did not flow down. Each sample was measured in triplicate.

Optimization using central composite design-response surface methodology

CCD-RSM was chosen to optimize gel formulation as this method required fewer experiments and could efficiently develop a second-order response model with two to six factors [14]. To screen the major factors for CCD-RSM, a series of single-factor experiments, including the amount of HM, P407, P188, and benzalkonium bromide, were conducted using gelling temperature as an index. Three-dimensional response surface plots were drawn according to the quadratic polynomial model, using Design-Expert software (version 10, Stat-Ease Inc., Minneapolis, MN, USA). We selected five representative formulations with a gelation temperature of 32°C to verify and evaluate the accuracy of the model.

Viscosity measurement of HM in situ gels

A viscometer with a no. 21 rotor was used to determine the viscosity of five optimized formulations in both gel and solution form. The speed was set at 1 rpm and 50 rpm for gel and solution, respectively.

Rectal retention test

Fifteen male SD rats were randomly divided into five groups (n = 3) to determine the rectal retention of the five optimized formulations. A gavage needle was employed to administer 0.2 mL of 0.5% methylene blue dye/HM gel (w/v) into the rectum 4 cm above the anus [15]. The color around the anus was then observed to determine whether the gel leaked from the anus. One rat in each group was killed by cervical dislocation at each time point (0.5 h, 2 h, and 6 h), and dissected to observe the dispersion and adherence of the HM gel in the rectum.

Establishment of the RP-HPLC analysis method of HM

The concentration of HM was determined using an RP-HPLC analysis system (Agilent 1260 series, Santa Clara, CA, USA). A Thermo Scientific™ (Waltham, MA, USA) Acclaim™ 120 C_{18} column (150 × 4.6 mm, 5 μm) was used for the separation. The mobile phase was composed of 40:60 methanol: 0.01 mol/L ammonium sulfate (v:v), and the flow rate and column temperature were set at 1.0 mL/min and 30°C, respectively. The detection wavelength was 320 nm. The injection volume of the sample was 10 μL. A 1.0 mg/mL of HM stock solution was obtained by dissolving 10.0 mg HM powder in 10 mL methanol. The HM stock solution was diluted with mobile phase to 200, 100, 50, 20, 10, 5, and 2.5 μg/mL. All solutions were analyzed as detailed above. Then, a linear regression between the HM concentration (C) and peak area (A) was conducted to obtain a standard curve. The precision and recovery of the RP-HPLC method was also evaluated.

In vitro release

The shaking method was used to determine the *in vitro* release profile of the HM gel [16]. A 100 mL conical flask containing 1.0 mL HM gel in solution form was placed in a 37°C air bath for 10 min until the solution was completely gelled. Then, 10 mL of pH 7.4 phosphate buffer was added as the release medium. The shaking speed was 50 rpm and the temperature was 37°C. At a specific time, 1.0 mL of release medium was removed for analysis and replaced with 1.0 mL fresh release medium. The samples were centrifuged at 10,000 rpm for 10 min, and the supernatants were collected to determine HM concentration by RP-HPLC. Finally, the amount of released HM was calculated, and the cumulative release curve was plotted.

Cell viability assay

CCK-8 assay was conducted to study the proliferation inhibition effect of HM gel on colon 26 cells. Briefly, colon 26 cells were seeded in 96-well cell culture plates at a density of 5×10^3 cells/well. After 24 h proliferation, cells were treated with HM, HM gel, and blank gel, respectively. Subsequently, 20 μL of CCK-8 reagent was added to each well and the cells were incubated at 37°C for 2 h. The optical density (OD) values were measured at 490 nm with 650 nm as the reference, using a Synergy H1 Microplate Reader (BioTek Instruments, Inc., VT, USA). The cell viability with no treatment was 100%. Cell viability was calculated using formula (1):

$$\text{Cell viability (\%)} = (OD_{test}\text{-}OD_{blank})/(OD_{control}\text{-}OD_{blank})*100\% \tag{1}$$

Annexin V-FITC/PI double-staining assay

For apoptosis analysis, the cells were stained using the Annexin V-FITC/PI double-staining assay (Annexin V-FITC/PI apoptosis detection kit). Colon 26 cells were seeded in a 6-well plate at a density of 1.5×10^5 cells/well and cultured at 37°C. After 24 h, cells were treated with either HM or HM gel at a concentration of 40 μg/mL HM, or blank gel. The cells were washed twice with PBS and collected for staining according to the manufacturer's instructions. The cells were then resuspended in 500 μL PBS for analysis using a FACSCalibur™ flow cytometer (BD Biosciences, Franklin Lakes, NJ, USA).

Wound healing assay

Colon 26 cells were seeded in 12-well plates at a density of 8×10^4 cells/well and cultured at 37°C and 5% CO_2. After 24 h, the confluent cell monolayer was wounded with a 200 μL pipette tip, washed with PBS, and exposed to either HM or HM gel at a concentration of 40 μg/mL HM, blank gel, or fresh medium (control group). Cells were immediately imaged under an inverted microscope as time point 0 h. The healing status of the scratch wound was observed and imaged again at 24 h.

Orthotopic cololon cancer model

Six-week-old BALB/c male mice were purchased from Beijing Vital River Laboratory Animal Technology Co., Ltd. (Beijing, China). All animal studies were approved by the Laboratory Animal Ethics Committee of the Institute of Materia Medica at the Institute of Materia Medica at the Chinese Academy of Medical Sciences (CAMS) and Peking Union Medical College (PUMC), and abided by national and institutional principles and protocols for the care and use of experimental animals. The model was performed as previously reported with some modifications [17]. Mice were fasted for 16 h before implantation, and then anesthetized with tribromoethanol (320 mg/kg) intraperitoneally [18]. Colon 26 cells (2×10^6 cells/100 μL/mouse) in logarithmic growth stage were inoculated intrarectally with an insulin needle inserted 1 cm into the anus of the mice. If the injection position of mice had an obvious bulge and no leakage, the model was considered successful.

Antitumor evaluation of HM in situ gels in vivo

When the tumor diameter reached approximately 0.5 cm, the tumor-bearing mice were randomized into four groups (n = 6): (1) control group: normal saline (0.2 mL) was injected by tail vein; (2) HM group: HM solution (30 mg/kg) was injected by tail vein; (3) blank gel group: blank gel (50 μL) was administered by rectal perfusion after anesthetization with tribromoethanol; and (4) HM gel group (30 mg/kg): HM gel was administrated by rectal perfusion after anesthetization with tribromoethanol. All groups were fasted for 24 h before drug dosing and the drug treatment was administered every three days for 12 days (5 doses total). At the end of the study, all mice were killed by cervical dislocation, and the organs and tumors excised and fixed with 4% neutral formaldehyde. Fixed organ tissues were paraffin embedded, stained with hematoxylin and eosin (H&E), and subjected to histopathological characterization. Apoptosis in tumor tissue was determined by terminal deoxynucleotidyl transferase-mediated dUTP nick end labeling (TUNEL) assay using a TUNEL-POD kit.

Survival analysis

Forty colon 26 tumor-bearing mice were randomly divided into four groups (n = 10): (1) control group: normal saline (0.2 mL) was injected by tail vein; (2) HM group: HM solution (30 mg/

kg) was injected by tail vein; (3) blank gel group: blank gel (50 μL) was administered by rectal perfusion after anesthetization with tribromoethanol; and (4) HM gel group (30 mg/kg): HM gel was administrated by rectal perfusion after anesthetization with tribromoethanol. All groups were fasted for 24 h before drug dosing and the drug treatment was administered every three days for 12 days (5 doses total). The first inoculation day was considered day 1, and the mice were monitored on a daily basis for up to 67 days until death. Survival curves were plotted according to the Kaplan-Meier method using GraphPad Prism software (version 5.0.0.0; GraphPad Software, San Diego, CA, USA, www.graphpad.com) [19].

Statistical analysis

Statistical analysis was conducted using SPSS software (version 4.0.100.1124; SPSS Inc., Chicago, IL, USA). Statistical comparisons were performed using one-way analysis of variance (ANOVA). Significant differences between two groups were evaluated by Student's t-test. Representative values are expressed as the mean ± standard deviation (SD). Asterisks indicate statistical significance as follows: $*P<0.05$, $**P<0.01$, $***P<0.001$.

Results and discussion

Optimization of the gel formulation

Thermosensitive gel is a commonly used preparation for mucosal administration. Polyoxyethylene/polyoxypropylene (PEO/PPO) block copolymers, such as P188 and P407, are the most widely used thermosensitive materials. Gelation temperature is a critical parameter for thermosensitive gels. The proportion of PEO and PPO segments, and the ratio of the selected copolymers effect gelation temperature, gel strength and bioadhesive force [20]. In order to increase the adhesion of drugs to the mucous membrane, it is necessary to add bioadhesive agents, such as HPMC, sodium carboxymethylcellulose (CMC-Na), alginate or other polymer materials [21]. The CCD-RSM, which integrates statistics and mathematics, has been commonly used for experiment optimization. CCD-RSM requires fewer tests, has high accuracy, and convenient application [22, 23]. In this study, we chose P407, P188, and HPMC as the gel matrix and

adopted CCD-RSM to optimize the ratio of essential ingredients, using the phase transition temperature as the evaluation index.

From our single factor experiments, the amounts of P407 and P188 had a greater influence on the gelation temperature than the amount of benzalkonium bromide or HM. With increased P407 concentration, the gelation temperature decreased, however, with increased P188 concentration, the gelation temperature increased (**Figure 1A**). Consequently, the amounts of P188, P407, and HPMC were chosen as variables to carry out the optimization. X1 represents the proportion of P188 (0% to 10%), X2 represents the proportion of P407 (18% to 22%), X3 represents the proportion of HPMC (0% to 1.2%), and T represents the calculated gelation temperature. The three variables (X1, X2, and X3) were designed at five levels: -1.732, -1, 0, 1, and 1.732. The experimental design and gelation temperature results are shown in **Table 1**. The quadratic polynomial regression of the relationship between the independent and dependent variables was carried out using Design-Expert 10 software (version 10.). The goodness of fit (R^2) and confidence (P) of the fitting equation were used as criteria for evaluating the model. The quadratic polynomial model was as follows: T = 43.32 + 5.40*X1-3.86*X2-0.44*X3 + 1.91*X1X2-0.41*X1X3-0.69*X2X3-1.34*X1^2 + 0.26*X2^2-0.21*X3^2 (R^2 = 0.9897, P<0.0001). The R^2 and *P* values indicate that the model was a good fit.

Three-dimensional effect surface diagrams were produced using Design-Expert 10 software according to the above quadratic polynomial [24]. As shown in **Figure 1B**, the gelation temperature decreased with increased P407 concentration, but increased with increased P188 concentration, in agreement with previous reports [25]. HPMC had no obvious effect on the gelation temperature, while P407 exhibited the greatest influence on the gelation temperature. Five alternative formulations with a gelation temperature of 32°C were selected to verify the established quadratic polynomial model. We chose 32°C as the gelation temperature for screening formulations in order to ensure that the gel is liquid at room temperature and gels rapidly at rectal temperature, which in humans normally ranges from 36.32-
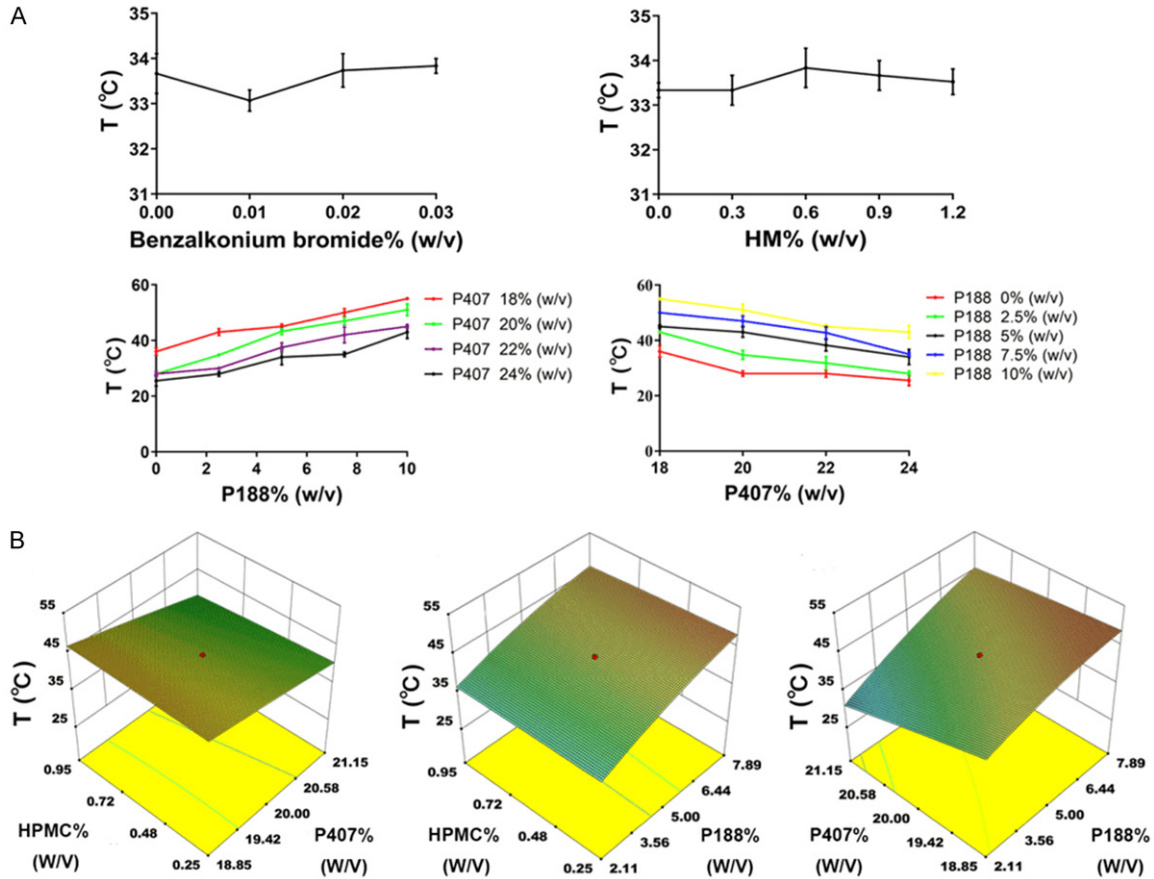
Figure 1. A. Effect of benzalkonium bromide, HM, P188 and P407 content on gelation temperature; data are expressed as mean ± SD (n = 6). B. Three-dimensional effect surface diagram of HM gel poltted by Design-Expert 10 software according to quadratic polynomial model.

37.76°C [26]. As shown in **Table 2**, the deviation between the measured value and the predicted value of the gelation temperature of each formulation was within 5%, indicating that the quadratic polynomial equation had good predictability. Therefore, the above five alternative formulations, were also the optimized formulations. To obtain the optimal formulation, the *in vivo* retention and *in vitro* release profiles were also determined (see below).

Viscosity measurement of the HM gel

Viscosity of thermosensitive gels is the key factor affecting the compliance and therapeutic effect of the drug [27] and therefore is a critical parameter for rheological characterization. High viscosity preparations are difficult to use and have poor compliance. However, low viscosity gels result in a short retention time of

the drug at the application site. We analyzed the viscosity of the gel using a rotational viscometer (SNB-1A, shanghai fangrui instrument CO., LTD). There was little difference in the gelation viscosity among the five formulations, though the viscosity of formulation 4 was slightly less than that of the other four formulations (**Table 3**).

Rectal retention test

Topical delivery systems require adequate structural strength to avoid detachment and breakage under *in vivo* conditions and to adhere properly to the mucous surface. A rectal retention test for the five optimized formulations was conducted in SD rats. As shown in **Table 4**, only formulation 4 leaked from the anus, while formulations 1, 2, 3, and 5 did not leak and were retained in the rectum for more than 6 h. Combined with the observed

Table 1. Central composite design results (mean ± SD, n = 3)

| No. | Levels of variables | | | Actual values of variables | | | Observed |
	X1	X2	X3	%P188 (w/v)	%P407 (w/v)	%HPMC (w/v)	T (°C)
1	-1	-1	-1	2.11	18.85	0.25	42.03 ± 0.25
2	+1	-1	-1	7.89	18.85	0.25	49.73 ± 0.30
3	-1	+1	-1	2.11	21.15	0.25	32.17 ± 0.28
4	+1	+1	-1	7.89	21.15	0.25	46.2 ± 0.35
5	-1	-1	+1	2.11	18.85	0.95	43.43 ± 0.35
6	+1	-1	+1	7.89	18.85	0.95	48.16±0.28
7	-1	+1	+1	2.11	21.15	0.95	30.2 ± 0.17
8	+1	+1	+1	7.89	21.15	0.95	43.2 ± 0.26
9	-1.732	0	0	0	20	0.6	28.96 ± 0.25
10	+1.732	0	0	10	20	0.6	50.2 ± 0.20
11	0	-1.732	0	5	18	0.6	48.00 ± 0.31
12	0	+1.732	0	5	22	0.6	37.73 ± 0.25
13	0	0	-1.732	5	20	0	43.5 ± 0.20
14	0	0	+1.732	5	20	1.2	42.47 ± 0.25
15	0	0	0	5	20	0.6	43.2 ± 0.17
16	0	0	0	5	20	0.6	43.3 ± 0.20
17	0	0	0	5	20	0.6	43.17 ± 0.28
18	0	0	0	5	20	0.6	43.5 ± 0.26
19	0	0	0	5	20	0.6	43.5 ± 0.10
20	0	0	0	5	20	0.6	43.23 ± 0.20

Note: P188, Poloxamer 188; P407, Poloxamer 407; HPMC, Hydroxypropyl methylcellulose.

anal retention times (**Figure 2**) this suggested the HM gel was retained for a sufficient amount of time to achieve therapeutically relevant levels of HM release and absorption.

RP-HPLC method for determining HM content

In order to determine the HM content, we developed a quantitative HPLC method. There was a good linear relationship between peak area (A) and HM concentration (C) between 2.5-200 μg/mL. The standard curve equation was A = 45.321C-12.834 (R^2 = 1). The RSD values of the low, medium, and high concentration samples were all less than 2.0%, and the average recovery was 98.79 ± 1.18% with an RSD of 1.20%, confirming the method is suitable for accurate quantitation of HM.

In vitro drug release profile of the HM gel

To examine the *in vitro* drug release profile of the HM gel we chose the shaking method, a membrane-less dissolution model, to better simulate the *in vivo* drug release mechanism

and kinetics of mucosal drug delivery. Based on the rectal retention test, formulations 1, 2, 3, and 5 were screened. As shown in **Figure 3**, HM released quickly from all formulations of HM gel in the first 2 h, and accumulation percentage exceeded 70% at 2 h. There was no significant difference in drug release behavior among the four formulations, which may be due to the water solubility of HM. Therefore, HM can be released and absorbed within the HM gel retention time. We chose formulation 5 as the optimal formulation for follow-up experiments as it was the most viscous and adhered to the rectum *in vivo* for the longest time. Four release models were used to mathematically fit the drug release curve of formulation 5 using DDsolver [28] software (version 1.0). The drug release behavior of the HM gel conformed to the Weibull release model (highest R^2 = 0.9961) (**Table 5**).

Inhibitory effect of HM gel on cell proliferation

We evaluated the inhibitory capacity of HM gel against colon 26 cell proliferation using the CCK-8 assay. Cell viability was >85% in all equivalent concentrations of HM tested, suggesting that the blank gel did not exhibit significant cytotoxicity and had good safety and biocompatibility (**Figure 4A**). With increased HM concentration, cell viability in the HM gel and HM groups decreased significantly (**Figure 4B**). The IC_{50} values of HM gel and HM were 34.63 μg/mL and 20.62 μg/mL, respectively.

In vitro, both HM gel and HM exhibited significant colon 26 cell cytotoxicity. The IC_{50} of HM was lower than that of HM gel, which may be related to the different uptake processes of HM gel and HM by colon 26 cells. Free HM is a small molecule with rapid cellular uptake.

Table 2. The prescription validation results (mean ± SD, n = 3)

Formulation	%HPMC (w/v)	%P188 (w/v)	%P407 (w/v)	Prediction of gel temperature (°C)	Measured gel temperature (°C)	Deviation (%)
1	0.68	2.28	21	32	31.90 ± 0.17	0.48
2	0.92	2.75	21.11	32	31.83 ± 0.28	0.80
3	0.33	2.11	21.15	32	31.96 ± 0.45	1.2
4	0.25	2.11	20.37	32	32.26 ± 0.35	0.69
5	0.93	2.13	20.7	32	31.9 ± 0.26	1.0

Note: P188, Poloxamer 188; P407, Poloxamer 407; HPMC, Hydroxypropyl methylcellulose; Deviation (%) = (predicted temperature-measured temperature)/predicted value × 100.

Table 3. Gel viscosity measurement results (mean ± SD, n = 3)

Formulation	1	2	3	4	5
Liquid viscosity (mPa/s)	89 ± 0.21	89 ± 0.13	89 ± 0.24	90 ± 0.11	90 ± 0.18
Gel viscosity (mPa/s)	3856 ± 0.31	3925 ± 0.15	3879 ± 0.22	3259 ± 0.21	3978 ± 0.24

Table 4. Leakage of HM gel loading (methylene blue dye visualization)

Formulation	1	2	3	4	5
Experimental mice (Numbers)	3	3	3	3	3
Mice with leakage (Numbers)	0	0	0	2	0

However, HM in gel formulation must be released from the gel before it is available for cellular uptake. Therefore, the cellular absorption of HM in HM gel is slower than that of free HM. However, as topical delivery HM gel should reduce systemic side effects and increase the efficacy of HM, we anticipated that HM gel would have greater efficacy than HM *in vivo*.

Inducing apoptosis effects of the HM gel

The role of HM in reducing apoptosis of various tumor cells has been widely studied by researchers. The results of a growing number of studies suggest that HM plays an important role in regulating a series of apoptosis modulator molecules (e.g. caspase, Bcl-2, p53, PARP, CAD, cyclin) [29-33]. HM can induce apoptosis of tumor cells by activating caspase-3, -8, -9 in both endogenous and exogenous apoptotic pathways [29], decreasing expression of Bcl-2 [30] and PARP [31], increasing p53 expression [29], and inhibiting the NF-κB signaling pathway [29]. In this study, the apoptosis inducing effect of HM was assessed in colon 26 cells (**Figure 5**). The blank gel did not induce apoptosis of colon 26

cells, as observed in the CCK-8 assay. After 24 h, compared with the control and blank gel groups, HM mainly induced late cellular apoptosis (upper right quadrant) of colon 26 cells. The late apoptotic cell ratio in the HM group was 22.67% ± 0.67%, which was slightly higher than that in the HM gel group (19.11% ± 1.61%). However, there was no significant difference in the ability to induce apoptosis between the HM gel and HM groups.

Inhibitory effect of HM gel on cell migration

The invasion and migration of tumor cells plays an important role in tumor metastasis. Migration ability is one of the main factors determining the malignancy of tumors. HM can mediate the ERK/CREB signaling pathway and inhibit invasion and metastasis of various malignant tumor cells by inhibiting the expression of epidermal growth factor (VEGF), matrix metalloproteinase (MMP) 2, and MMP 9 [34, 35]. In addition, HM inhibits the proliferation, migration, and invasion of tumor cells by inhibiting the expression of TGF-β pathway-related proteins and epithelial-mesenchymal transition (EMT) [36].

The wound healing test is used to assess cell plane migration and the movement characteristics of tumor cells. In this study, this method was used to establish cell injury healing *in vitro* and to observe cell migration. In this study, after 24 h the control and blank gel groups scratch was completely populated with cells, while in the HM and HM gel groups the
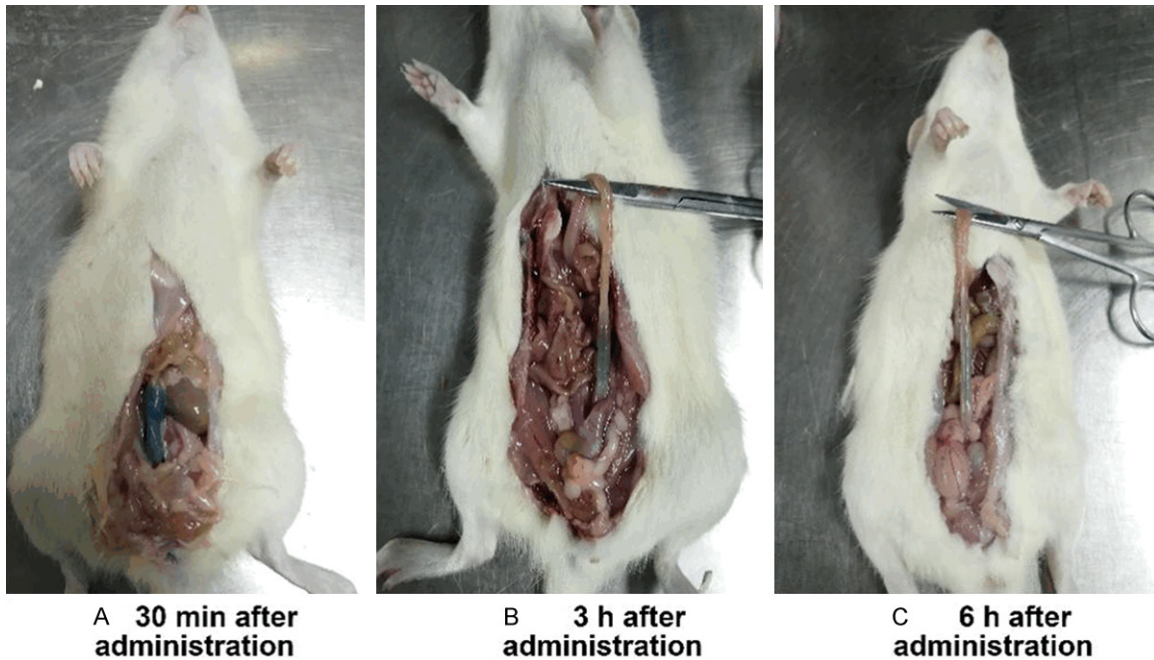
Figure 2. Gel retention in rectum of rats at different times; 0.5% methylene blue dye/HM gel (w/v) into the rectum 4 cm above the anus.
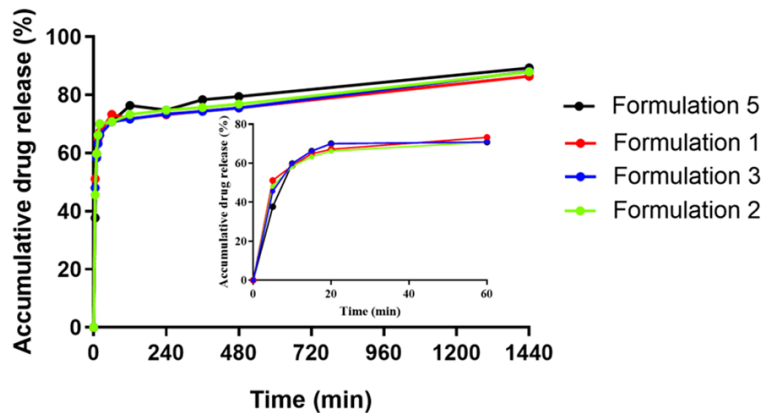

Figure 3. In vitro release profile of HM gel determined by shaking method in PBS (pH 7.4) at 37°C.

scratch was narrow but still visible (**Figure 6**). In addition, the cell density in the HM and HM gel groups decreased and the intercellular space between cells increased, indicating that HM could significantly inhibit the migration ability of colon 26 cells. This suggests that HM gel may have an anti-metastatic effect.

In vivo antitumor effect of HM gel

The body weight of tumor-bearing mice increased in all treatment groups. In detail, the control group gained the most weight, followed by the blank gel group, HM gel group, and HM group (**Figure 7A**). Mice in the HM group manifested minor convulsions during drug administration, indicating acute toxicity of HM intravenous injection in mice. Conversely, mice in the HM gel group did not show any discomfort during gel administration. There were no obvious histopathological abnormalities in the HM gel group after several rectal perfusions (**Figure 7E**). Based on these results, HM gel was well tolerated in mice and may be less toxic than intravenous HM therapy.

Monitoring tumor volume in real-time was difficult because of the deep anatomical position of the tumors. Therefore, we recorded the weight of dissected tumor tissues at the end of the study. The HM gel group exhibited the strongest inhibitory effect among all groups, and there was a significant difference between the two HM groups and the control

Table 5. Fitting results of *in vitro* release of Formulation 5

Release model	Equation	Fit result	Good-ness of fit (R^2)
Peppas-Sahlin	$F = k_1*t\textasciicircum m+k_2*t\textasciicircum(2*m)$	$F = 49.46*t\textasciicircum 0.098-2.7*t\textasciicircum(2*0.098)$	0.9650
Higuchi	$F = k_H*t\textasciicircum 0.5$	$F = 3.624*t\textasciicircum 0.5$	0.6640
First-order	$F = 100*[1-Exp(-k_1*t)]$	$F = 100*[1-Exp(-0.074*t)]$	0.9511
Weibull	$F = 100*\{1-Exp[-((t-Ti)\textasciicircum β)/α]\}$	$y = 100*\{1-Exp[-((t-4.9895)\textasciicircum 0.117)/1.25]\}$	0.9961
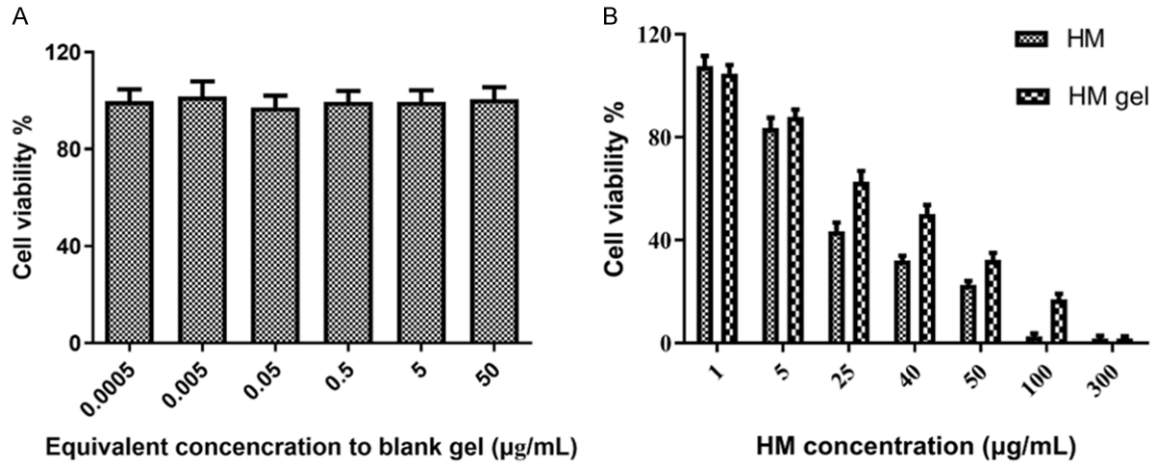
Figure 4. CCK-8 assay results of colon 26 cells; data are expressed as mean ± SD (n = 4). A. Cytotoxicity of blank gel after incubation for 24 h. B. Cell viability of HM group and HM gel group after incubation for 24 h.
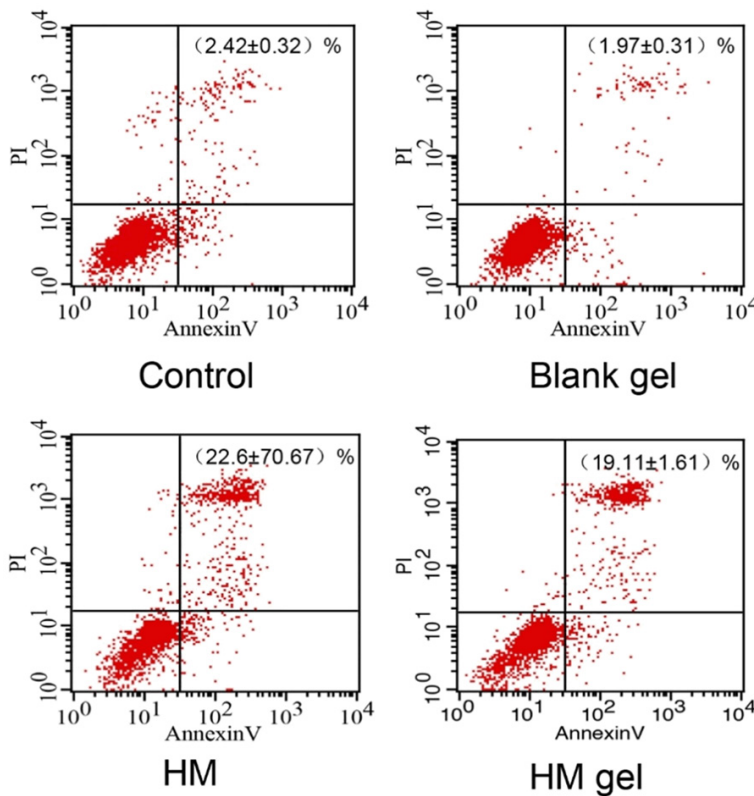

Figure 5. Quantitative apoptosis assay of colon 26 cells induced by HM gel after 24 h incubation (upper right quadrant: late cellular apoptosis); date are expressed as mean ± SD (n = 3).

group (**P<0.01). In particular, the HM gel group exhibited a more significant inhibition effect than the HM group (*P<0.05) (**Figure 7B** and **7C**).

To assess the tumor inhibitory effect at the cellular level, we used a TUNEL assay to measure apoptosis and necrosis in the tumor tissues (**Figure 7D**). In the HM gel group tumors, most of the tumor cells were apoptotic. Furthermore, apoptotic cells were also present inside the tumor, implying that the HM in the HM gel could penetrate the tumor tissue. Conversely, in the HM group, far less cells were apoptotic, and almost no apoptosis occurred in the control and blank gel groups. This result was in accordance with the anti-tumor results and demonstrated that the enhanced anti-cancer effect of HM gel was due to induction of apoptosis.

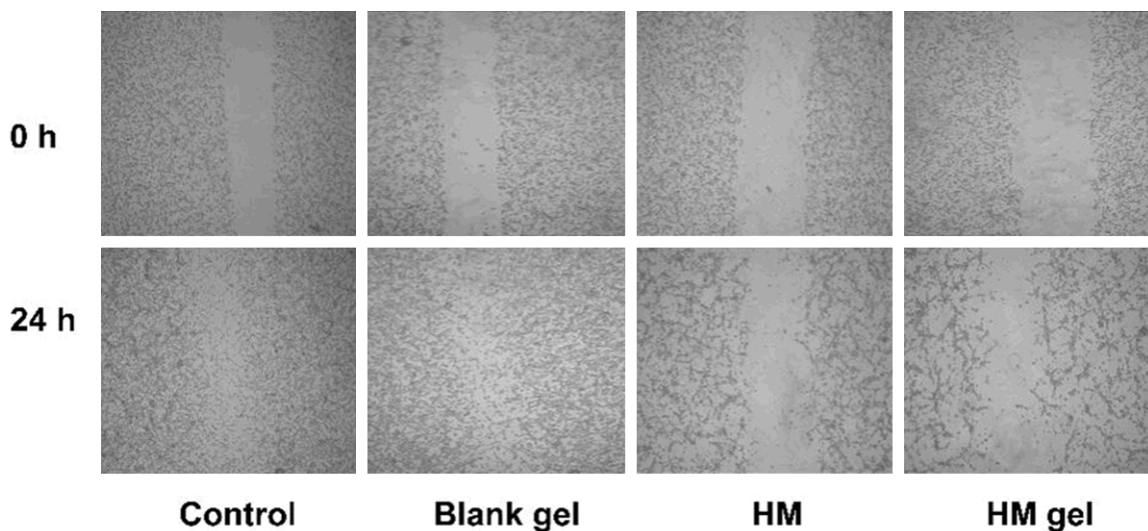**Figure 6.** Cell wound scratch assay images observed under microscope after treatment with HM gel (magnification × 40) for 0 h and 24 h.

The dissected organs were paraffin embedded and stained with H&E to investigate the anti-metastatic abilities of HM gel in colon 26 tumor-bearing mice. The pathological images of the lungs are shown in **Figure 7F**. In the lung tissue of the control group and blank gel group there was evidence of metastatic loci and vascular invasion (red arrows), while there was no metastasis in the lungs of the HM gel and HM groups. In addition, severe edema, hypertrophic lung interval, and reduced alveolar structure were observed in the lungs of the control, blank gel, and HM treatment groups, while these phenomena were not apparent in the lungs of the HM gel group. The other organs examined (liver, kidney, spleen, heart, and brain) exhibited no apparent abnormalities under H&E staining. This suggests that *in situ* administration of HM gel can effectively inhibit the metastasis and growth of colon 26 cells in lung tissues.

Survival analysis

Based on the above effective inhibition effect on tumor growth in vitro and in vivo, we further evaluated the influence of HM gel on the survival time of colon 26 tumor-bearing mice. As shown in **Figure 8**, both HM gel and HM treatment can prolong the survival period of tumor-bearing mice. Log-rank analysis showed that the median survival times of the HM gel, HM, control, and blank gel groups were 55, 46,

35, and 35 days post inoculation, respectively. The median survival time of the HM and HM gel groups was significantly higher than that of the control and blank gel groups. More importantly, the HM gel group had a significantly longer median survival time than that of the HM group (**P<0.01), which indicated that HM gel both enhances the drug effect and reduces the systemic toxicity of HM.

Conclusions

In order to achieve efficient drug delivery and reduce systemic toxicity, we formulated a HM gel for local drug delivery. The HM gel had good rheological and release properties, and was retained for more than 6 h in the rectum. Most importantly, HM gel exhibited inhibitory effects on cell proliferation and migration in vitro by inducing late apoptosis. Benefiting from topical administration, HM gel improved the accumulation of HM in tumor sites after rectal perfusion, which led to the effective inhibition of orthotopic colon 26 tumor growth and its distant metastasis, and therefore prolonged survival time. Thus, HM gel is a promising HM delivery strategy for treating colorectal cancer.
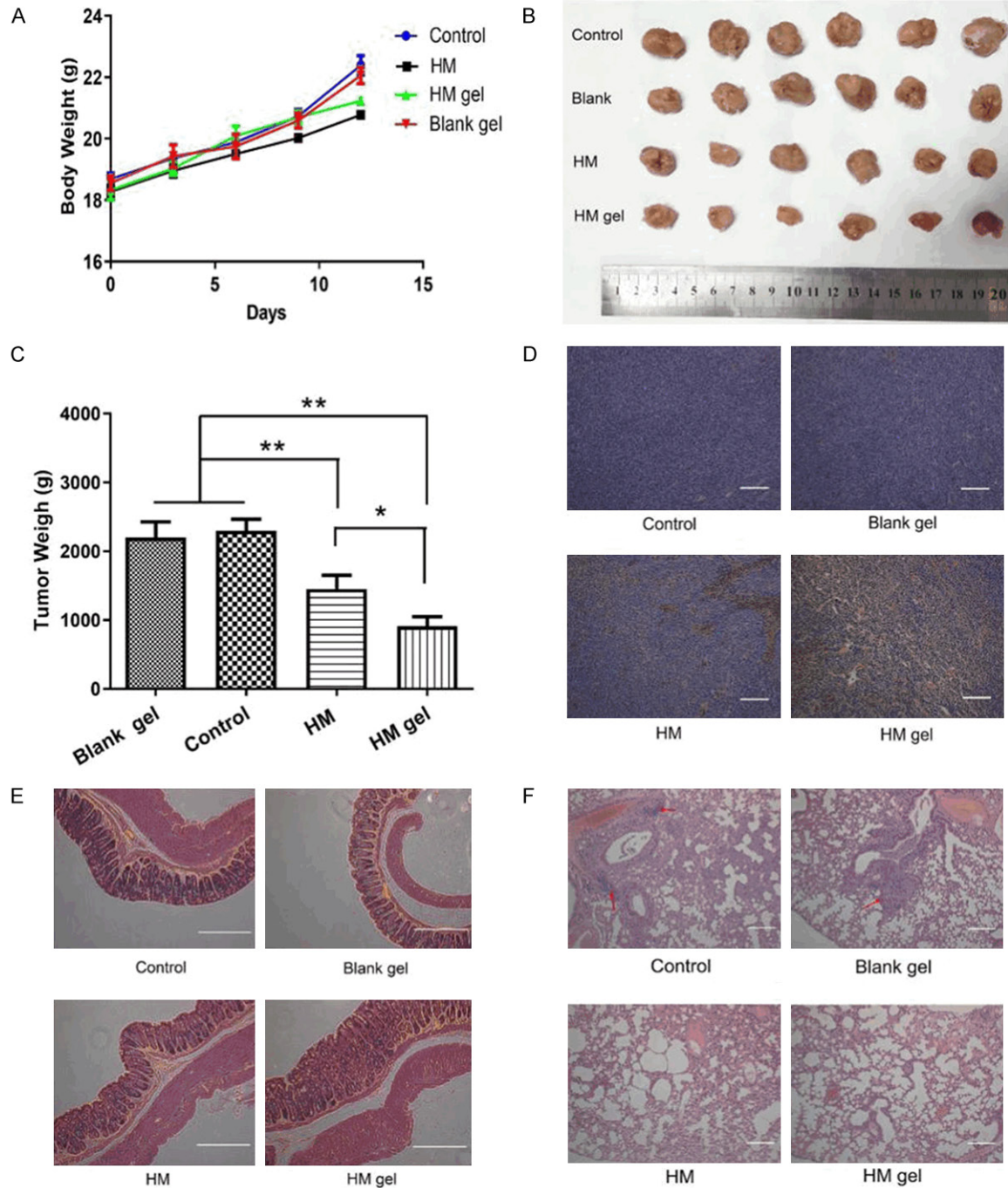
Acknowledgements

Figure 7. Anti-tumor activity of HM gel in orthotopic colon 26 tumor-bearing BALB/c mice; control group: normal saline (0.2 mL) was injected by tail vein; HM group: HM solution (30 mg/kg) was injected by tail vein; blank gel group: blank gel (50 μL) was administrated by rectal perfusion after anesthetization with tribromoethanol; HM gel group (30 mg/kg): HM gel was administrated by rectal perfusion after anesthetization with tribromoethanol. A. Changes in body weight in mice during the experiment; data are expressed as mean ± SD (n = 6). B. The photo of tumor tissues in each group at the end of treatment (n = 6). C. Tumor weight calculated 12 days after administration of normal saline, blank gel, HM and HM gel; data are expressed as mean ± SD (n = 6); **P<0.01, HM gel versus control and Blank gel; **P<0.01, HM versus control and blank gel; *P<0.05, HM gel versus HM. D. Paraffin-embedded tumor sections after TUNEL (the apoptotic cells are shown in brown); scale bar =120 μm, magnification × 100. E. H&E assay of colorectal in each group; scale bar = 120 μm, magnification × 100. F. H&E assay of lungs in each group. Red arrows indicate the tumor metastasis loci in the lungs; scale bar = 120 μm, magnification × 100.
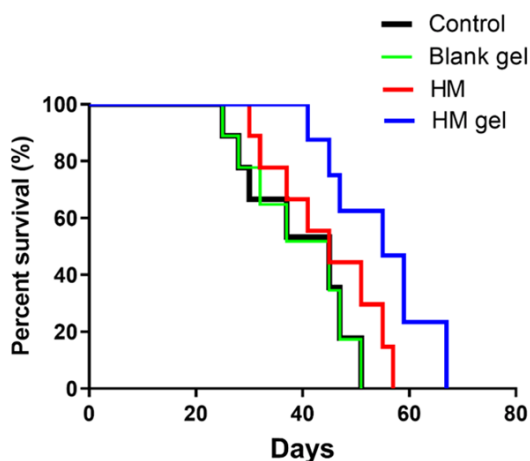
Figure 8. Kaplan-Meier survival curves of colon 26 tumor-bearing BALB/c mice (n = 10); the day on which colon 26 cells were inoculated in mice was considered as the first day, and the mice were monitored for 67 days on a daily basis; *P<0.05, HM versus control and Blank gel; **P<0.01, HM gel versus control and Blank gel; **P<0.01, HM versus HM gel.

Disclosure of conflict of interest

None.

Address correspondence to: Wei Huang and Zhonggao Gao, State Key Laboratory of Bioactive Substance and Function of Natural Medicines, Department of Pharmaceutics, Institute of Materia Medica, Chinese Academy of Medical Sciences and Peking Union Medical College, Beijing 100050, China. Tel: +86-10-6302-6505; E-mail: huangwei@imm.ac.cn (WH); Tel: +86-10-6302-8096; E-mail: zggaoimm@126.com (ZGG); Xuezhong Xing, National Cancer Center/National Clinical Research Center for Cancer/Cancer Hospital, Chinese Academy of Medical Sciences and Peking Union Medical College, Beijing 100021, China. Tel: +86-10-8778-8257; E-mail: xingxuezhong@cicams.ac.cn; Jianguo Xing, Xinjiang Key Laboratory of Uighur Medicines, Xinjiang Institute of Materia Medica, Urumqi 830004, China. Tel: +86-991-2300682; E-mail: xingjg@126.com

References

[1] Liu AY, Qiao JT, He LY, Liu ZM, Chen JC, Pei FH and Du YJ. Nitrogen permease regulator-like-2 exhibited anti-tumor effects and enhanced the sensitivity of colorectal cancer cells to oxaliplatin and 5-fluorouracil. Onco Targets Ther 2019; 12: 8637-8644.

[2] Rubinstein A. Approaches and opportunities in colon-specific drug delivery. Crit Rev Ther Drug Carrier Syst 1995; 12: 101-149.

[3] Shen N, Hu J, Zhang LN, Zhang L, Sun YG, Xie YH, Wu SM, Liu L and Gao ZB. Doxorubicin-loaded zein in situ gel for interstitial chemotherapy of colorectal cancer. Acta Pharm Sin B 2012; 2: 610-614.

[4] Tabrizizadeh M, Kazemipoor M, Hakimian M, Maleksabet M, Kazemipoor M, Zandi H, Pourrajab F, Che C and Cordell G. Effects of a Peganum harmala (Zygophyllaceae) preparation for root canal disinfection. Phytother Res 2018; 32: 672-677.

[5] Filali I, Bouajila J, Znati M, Garah B and Jannet HB. Synthesis of new isoxazoline derivatives from harmine and evaluation of their anti-Alzheimer, anti-cancer and anti-inflammatory activities. J Enzyme Inhib Med Chem 2014; 30: 371-376.

[6] Chen Q, Ma K, Wang ZY and Ding QQ. Harmine induces gastric cancer cell apoptosis through the ROSmediated PI3K/AKT signaling pathway. Curr Signal Transduction Ther 2015; 10: 112-118.

[7] Jiménez J, Riverón-Negrete L, Abdullaev F, Espinosa-Aguirre J and Rodríguez-Arnaiz R. Cytotoxicity of the β-carboline alkaloids harmine and harmaline in human cell assays in vitro. Exp Toxicol Pathol 2008; 60: 381-389.

[8] Louis ED and Zheng W. Beta-carboline alkaloids and essential tremor: exploring the environmental determinants of one of the most prevalent neurological diseases. ScientificWorldJournal 2010; 10: 1783-1794.

[9] Wang J, Zhou HC, Zheng QX, Yan J, Liu P, Li GH, Zhang XF and Tang HY. Synthesis of pH-sensitive, water-soluble paclitaxel prodrugs based on norbornene-functional polylactide by copper-free click chemistry. Int J Polym Mater Polym Biomater 2016; 65: 789-796.

[10] Halligan SC, Dalton MB, Murray KA, Dong Y, Wang W, Lyons JG and Geever LM. Synthesis, characterisation and phase transition behaviour of temperature-responsive physically crosslinked poly (N-vinylcaprolactam) based polymers for biomedical applications. Mater Sci Eng C Mater Biol Appl 2017; 79: 130-139.

[11] Choi HG, Jung JH, Ryu JM, Yoon SJ, Oh YK and Kim CK. Development of in situ-gelling and mucoadhesive acetaminophen liquid suppository. Int J Pharm (Amsterdam, Neth) 1998; 165: 33-44.

[12] Ur-Rehman T, Tavelin S and Gröbner G. Chitosan in situ gelation for improved drug loading and retention in poloxamer 407 gels. Int J Pharm 2011; 409: 19-29.

[13] Jin R, Moreira Teixeira LS, Dijkstra PJ, Karperien M, van Blitterswijk CA, Zhong ZY and Feijen J. Injectable chitosan-based hydrogels for cartilage tissue engineering. Biomaterials 2009; 30: 2544-2551.

[14] Duan YW, Cai XQ, Du HL and Zhai GX. Novel in situ gel systems based on P123/TPGS mixed micelles and gellan gum for ophthalmic delivery of curcumin. Colloids Surf B Biointerfaces 2015; 128: 322-330.

[15] Yuan Y, Cui Y, Zhang L, Zhu HP, Guo YS, Zhong B, Hu X, Zhang L, Wang XH and Chen L. Thermosensitive and mucoadhesive in situ gel based on poloxamer as new carrier for rectal administration of nimesulide. Int J Pharm 2012; 430: 114-119.

[16] Yang Y, Wang JC, Zhang X, Lu WL and Zhang Q. A novel mixed micelle gel with thermo-sensitive property for the local delivery of docetaxel. J Control Release 2009; 135: 175-182.

[17] Takahashi T, Morotomi M and Nomoto K. A novel mouse model of rectal cancer established by orthotopic implantation of colon cancer cells. Cancer Sci 2004; 95: 514-519.

[18] Lee MR, Suh HR, Kim MW, Cho JY, Song HK, Jung YS, Hwang DY and Kim KS. Comparison of the anesthetic effects of 2,2,2-tribromoethanol on ICR mice derived from three different sources. Lab Anim Res 2018; 34: 270-278.

[19] Wang X, Bai F, Pang H and George SL. Bias-adjusted Kaplan-Meier survival curves for marginal treatment effect in observational studies. J Biopharm Stat 2019; 29: 592-605.

[20] Swain GP, Patel S, Gandhi J and Shah P. Development of Moxifloxacin Hydrochloride loaded in-situ gel for the treatment of periodontitis: in-vitro drug release study and antibacterial activity. J Oral Biol Craniofac Res 2019; 9: 190-200.

[21] Genç L, Oğuzlar C and Güler E. Studies on vaginal bioadhesive tablets of acyclovir. Pharmazie 2000; 55: 297-299.

[22] Huang WW, Zhang N, Hua HY, Liu TB, Tang YF, Fu LL, Yang YN, Ma XJ and Zhao YX. Preparation, pharmacokinetics and pharmacodynamics of ophthalmic thermosensitive in situ hydrogel of betaxolol hydrochloride. Biomed Pharmacother 2016; 83: 107-113.

[23] Xu D, Zhu W, Jiang Y, Li XS, Li WN, Cui JC, Yin JX and Li GT. Rational design of molecularly imprinted photonic films assisted by chemometrics. J Mater Chem 2012; 22: 16572-16581.

[24] Bei YY, Zhou XF, You BG, Yuan ZQ, Chen WL, Xia P, Liu Y, Jin Y, Hu XJ, Zhu QL, Zhang CG, Zhang XN and Zhang L. Application of the central composite design to optimize the preparation of novel micelles of harmine. Int J Nanomedicine 2013; 8: 1795-1808.

[25] Akl MA, Ismael HR, Abd Allah FI, Kassem AA and Samy AM. Tolmetin sodium-loaded thermosensitive mucoadhesive liquid suppositories for rectal delivery; strategy to overcome oral delivery drawbacks. Drug Dev Ind Pharm 2019; 45: 252-264.

[26] Geneva II, Cuzzo B, Fazili T and Javaid W. Normal body temperature: a systematic review. Open Forum Infect Dis 2019; 6: ofz032.

[27] Chen MJ, Cheng YM, Lai PH, Wu JF and Hsu YC. In vitro biocompatibility of thermally gelling liquid mucoadhesive loaded curcuminoids in colorectal cancer chemoprevention. Int J Colorectal Dis 2012; 27: 869-878.

[28] Zhang Y, Huo M, Zhou J, Zou A, Li W, Yao C and Xie S. DDSolver: an add-in program for modeling and comparison of drug dissolution profiles. AAPS J 2010; 12: 263-271.

[29] Hamsa TP and Kuttan G. Harmine activates intrinsic and extrinsic pathways of apoptosis in B16F-10 melanoma. Chin Med 2011; 6: 11.

[30] Cao MR, Li Q, Liu ZL, Liu HH, Wang W, Liao XL, Pan YL and Jiang JW. Harmine induces apoptosis in HepG2 cells via mitochondrial signaling pathway. Hepatobiliary Pancreat Dis Int 2011; 10: 599-604.

[31] Dai F, Chen Y, Song Y, Huang L, Zhai D, Dong Y, Lai L, Zhang T, Li D, Pang X, Liu M and Yi Z. A natural small molecule harmine inhibits angiogenesis and suppresses tumour growth through activation of p53 in endothelial cells. PLoS One 2012; 7: e52162.

[32] Liu J, Wu Q, Wang Z, Hong Q, Wang J, Han B, Fan C and Tian M. Harmine-inducing apoptosis of jurkat leukemia cells and its mechanism in vitro. Guangming J Chin Med 2012; 27: 242-244.

[33] Song Y, Kesuma D, Wang J, Deng Y, Duan J, Wang JH and Qi RZ. Specific inhibition of cyclin-dependent kinases and cell proliferation by harmine. Biochem Biophys Res Commun 2004; 317: 128-132.

[34] Gao J, Zhu H, Wan H, Zou X, Ma X and Gao G. Harmine suppresses the proliferation and migration of human ovarian cancer cells through inhibiting ERK/CREB pathway. Oncol Rep 2017; 38: 2927-2934.

[35] Hamsa T and Kuttan G. Studies on anti-metastatic and anti-invasive effects of harmine using highly metastatic murine B16F-10 melanoma cells. J Environ Pathol Toxicol Oncol 2011; 30: 123-137.

[36] Wang ML, Niu JL, Gao Y, Wang YP, Zhang LF, Zhang Y and Wang P. Effects of harmine on the proliferation, migration and invasion of human breast cancer MCF7 cells. J Chin Med Mater 2018; 41: 1702-1706.